

Real-time imaging of vertically aligned carbon nanotube array growth kinetics

A A Puretzky, G Eres, C M Rouleau, I N Ivanov and D B Geohegan

Oak Ridge National Laboratory, Oak Ridge, TN 37831-6056, USA

E-mail: puretzkya@ornl.gov

Received 14 October 2007, in final form 4 December 2007

Published 14 January 2008

Online at stacks.iop.org/Nano/19/055605

Abstract

In situ time-lapse photography and laser irradiation are applied to understand unusual coordinated growth kinetics of vertically aligned carbon nanotube arrays including pauses in growth, retraction, and local equilibration in length. A model is presented which explains the measured kinetics and determines the conditions for diffusion-limited growth. Laser irradiation of the growing nanotube arrays is first used to prove that the nanotubes grow from catalyst particles at their bases, and then increase their growth rate and terminal lengths.

 Supplementary data files are available from stacks.iop.org/Nano/19/055605

 This article features online multimedia enhancements

(Some figures in this article are in colour only in the electronic version)

1. Introduction

Self-assembly of carbon nanotubes into vertically aligned arrays during chemical vapor deposition (CVD) is currently of great interest because of their rapid, cooperative growth mechanism [1–5] and the potential macroscopic applications of multi-millimeter-long aligned nanotubes [6–9]. The length of these arrays is currently limited to a few millimeters (occasionally more than a centimeter [10]). One of the possible approaches to maximize array length, growth rate, and quality is to combine *in situ* measurements of their growth modes during nucleation, growth to long lengths, and termination and *ex situ* characterization to understand the major factors that limit the growth.

In situ observations of growth of individual carbon nanotubes during CVD using electron microscopy [11–15] and vertically aligned carbon nanotube arrays (VANTAs) using optical techniques [4, 16, 17] have generated most of the new insights for understanding the mechanisms responsible for their growth. As a result, new growth models have been developed to explain the activation energies and main processes responsible for the observed kinetics, growth termination, and number of walls of the nanotubes in the arrays under different growth conditions [4, 5].

However, these models focus on isolated catalyst nanoparticles growing individual carbon nanotubes and do

not take into account interactions within an entangled mat of growing nanotubes. For example, the models do not explain why nanotube arrays grow cooperatively during CVD and maintain relatively flat surfaces throughout nucleation, growth, and growth termination. Moreover, although it is clear that in many CVD experiments nanotubes grow from their ‘base’, i.e. from catalyst nanoparticles attached to the substrate [18–20], the rapid growth of dense nanotube arrays (nanotubes spaced ~15–30 nm apart) to multi-millimeter heights appears to disagree with expectations for diffusion-limited growth [1].

In this paper we report cooperative phenomena in VANTA growth observed by real-time imaging using remote microscope videography combined with pulsed laser irradiation to identify and alter the growth mode of the nanotubes.

2. Experimental details

The experimental apparatus used for CVD of VANTAs is identical to that described in [4, 16]. The Si(100) substrates (coated with electron-beam evaporated metal multilayer films (10 nm of Al, 0.2 nm of Mo, and 1 nm of Fe)) were mounted vertically in a horizontal, 3 inch-diameter, quartz tube CVD reactor using a quartz mount. The substrates were turned parallel to the tube axis such that the wafers

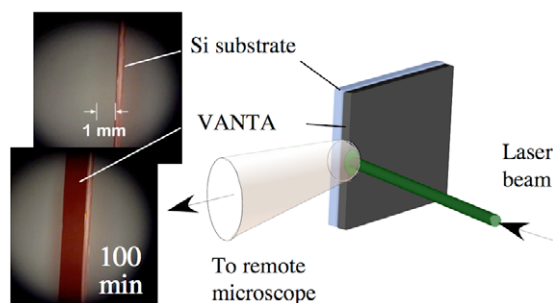


Figure 1. Schematic diagram of imaging and laser irradiation during growth of VANTA. Beam geometry and imageable area are indicated. Two frames showing the edge of a Si substrate before growth (top) and carbon nanotube arrays after 100 min of growth (bottom) are shown at the left.

could be viewed side-on from the end windows of the quartz tube. This substrate orientation permitted laser irradiation of the growing arrays by the introduction of a laser beam through a small opening in the furnace (figure 1, see also S1 (available at stacks.iop.org/Nano/19/055605)). First, the catalyst films were pre-treated in flowing Ar (2000 sccm)/H₂ (400 sccm) at atmospheric pressure and 730 °C for 10 min. Then a pre-established flow of C₂H₂ was introduced into the flowing Ar/H₂ gas mixture that resulted in VANTA growth. The length of the arrays was directly measured by videography using a remote microscope (Questar, QM-1, resolution ~5 μm) with long (100 cm) working distance using a camcorder (Sony DCR-TRV350) operated in either regular (30 frames s⁻¹) or time interval (2 s recording time every 30 s) recording modes as shown in figure 1 (see also S1 (available at stacks.iop.org/Nano/19/055605)).

3. Results and discussion

3.1. Laser irradiation during growth: base versus tip growth

To determine if the nanotube arrays grow from catalyst nanoparticles at their ‘base’ or their ‘tip’, laser irradiation and imaging were performed simultaneously. Five sequences of Nd:YAG laser pulses (1 Hz, 50 shots each, energy densities in a range from 1.1 to 4.6 J cm⁻²) were used to ablate the top surface of the array sufficient for visible damage observed through the microscope, thereby ensuring that any catalyst nanoparticles at the tips of the nanotubes were removed. Frame-by-frame measurements from the time-lapse movie of the experiment reveals that laser irradiation removes approximately 50–100 μm of length. However, following laser irradiation in each case the array is observed to grow faster, more than compensating for the loss in length due to ablation. Figure 2(a) shows a sequence of frames from the corresponding movie demonstrating the laser ablation plume at 36 min of growth, recession in length due to ablation (37 min), and continuation of growth to length longer than the starting unirradiated array (126 min) (the corresponding length versus time, $R(t)$ plot, is shown in figure S3b (available at stacks.iop.org/Nano/19/055605)). The scanning electron micrographs of the irradiated regions in figures 2(b)

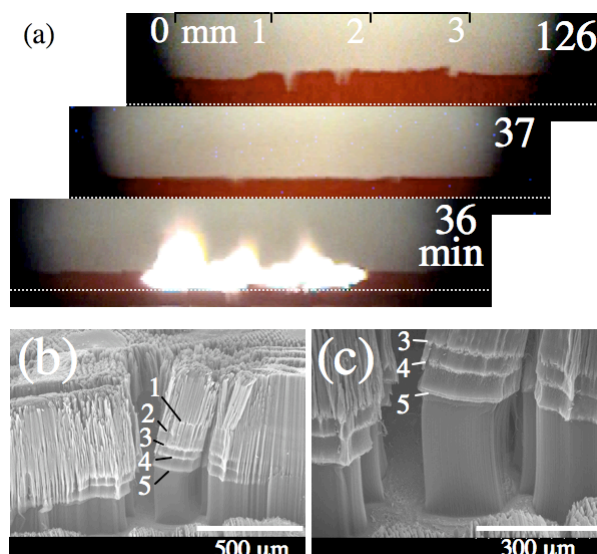


Figure 2. (a) A sequence of frames (from 36 to 126 min) taken from a movie of VANTA array growth (available at stacks.iop.org/Nano/19/055605). The frame at 36 min shows the laser ablation plume resulting from laser irradiation of VANTA during growth using the following Nd:YAG laser parameters: $\lambda = 1.06 \mu\text{m}$, 10 ns pulse width, 1 Hz repetition rate, 6 mm beam spot. Five irradiation sequences were performed at different times during growth at: (1) 27 min (50 pulses, 1.1 J cm⁻²), (2) 32 min (600 pulses, 1.1 J cm⁻²), (3) 36 min (50 pulses, 2.5 J cm⁻²), (4) 39 min (50 pulses, 3.6 J cm⁻²), and (5) 42 min (50 pulses, 4.6 J cm⁻²). (b), (c) SEM images of VANTA irradiated during growth. The laser modified tubes at the top and ‘the new growth’ at the bottom of the array can be clearly seen from these images. The horizontal bands marked as 1–5 correspond to the five subsequent irradiation events.

and (c) show bright bands corresponding to the five sequential irradiation events performed at different times during growth: (1) at 27 min (50 pulses, 1.1 J cm⁻²), (2) 32 min (600 pulses, 1.1 J cm⁻²), (3) 36 min (50 pulses, 2.5 J cm⁻²), (4) 39 min (50 pulses, 3.6 J cm⁻²), and (5) 42 min (50 pulses, 4.6 J cm⁻²), which are interpreted as the position of the substrate–array interface during the laser treatments, indicating that the whole length of the nanotube array was heated by the laser beam to the catalyst at their bases. The only undamaged nanotubes are present at the base of the array and correspond to the growth region that occurred after the final laser irradiation, clearly indicating that growth occurs from the base of the nanotubes. The base growth implies that the feedstock molecules should diffuse through the array to reach the catalyst nanoparticles at the bottom of the array, which could limit the ultimate length of VANTAs in addition to growth termination due to decreased catalyst activity.

3.2. Cooperative growth of VANTAs

In situ videography shows that VANTA growth is a complex cooperative process, with regional pauses, retraction, and growth spurts working in a coordinated fashion in the array until a typically sudden termination. For example, figure 3(a) shows a length versus time, $R(t)$, plot measured from images along a 1 mm region of a VANTA during

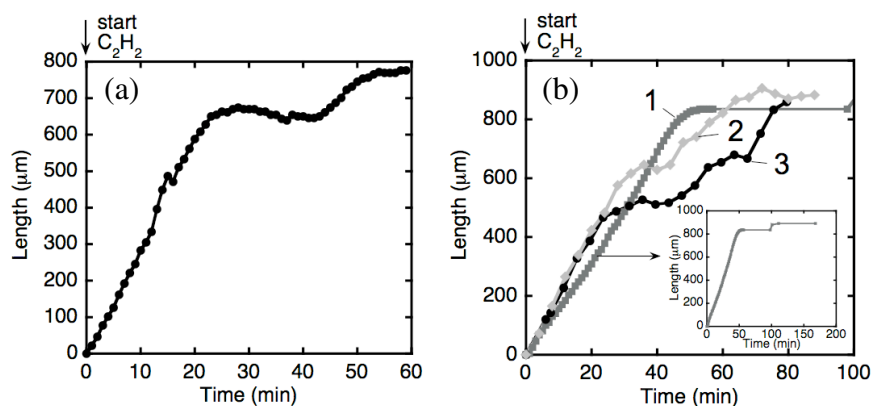


Figure 3. (a) Length of a nanotube array versus time, $R(t)$ plot. The growth conditions were as follows: gas flows, Ar (2000 sccm), H_2 (400 sccm), C_2H_2 (2.4 sccm); total pressure, 750 Torr; growth temperature, 730 °C. (b) Three $R(t)$ plots obtained from different experimental runs (curves 1–3) using the same growth conditions as in (a). The inset shows long time behavior of run 1.

growth (see also the corresponding short movie, S2 (available at stacks.iop.org/Nano/19/055605)). The resulting growth kinetics of the nanotube array can be described by four different stages. First, from 0 to 20 min VANTAs grow linearly from 0 to 0.7 mm at a rate of $0.5 \mu\text{m s}^{-1}$. Next the growth rate decreases and appears to stop at $t = 28$ min. However, this region of decreasing growth rate continues from $t = 28$ to 41 min as the array height actually decreases slightly. During this growth pause/retraction, other regions of the array continue to grow and ‘catch up’ to produce a more level array. In the third stage of growth from $t = 41$ to 49 min, the lower part of the array increases in length while the upper part apparently stopped. In the fourth stage, during resumption of growth, the growth of the entire array terminates rather suddenly (see S2, available at stacks.iop.org/Nano/19/055605).

Different growth runs display variations of these effects. For example, the kinetics for three different runs under identical conditions shown in figure 3(b) all exhibit regions of a linear growth stage, sudden termination of the growth, and spontaneous regrowth after some induction time. In some of these cases, two pauses were observed in the growth (figure 3(b), curve 3), and sometimes the growth restarts only after long (50 min) periods (see the inset in figure 3(b)).

While the mechanisms of coordinated growth are not yet clear, it is reasonable to assume that differences in growth rates and growth termination of some fraction of the tubes inside the entangled array lead to both stretched and kinked nanotubes (i.e. tensile and compressive strain). As significant fractions of nanotubes in the array stop growing, the compressive stress in the array results in the observed retraction. *Ex situ* stress–strain characteristics of carbon nanotube arrays were studied in [9]. It was concluded that the stress–strain behavior of the nanotube arrays is similar to that of flexible open-cell foam structures. This stress may help to maintain the flatness of the top surface of the array by removing the length non-uniformities as observed in the videos.

3.3. Growth limitation due to feedstock diffusion

The constant growth rates during the first 0.5–0.8 mm of height (figures 3(a) and (b)) imply that the growth under these

conditions is not diffusion limited (see also the $R(t)$ plots in figures 3S a, b (available at stacks.iop.org/Nano/19/055605)). However, at lower C_2H_2 partial pressures quite different growth kinetics are observed. A set of contrast-enhanced digital images extracted from a movie of the VANTA growth using a factor of two lower feedstock gas flow (1.2 sccm) is presented in figure 4(a), and the progression in height at the indicated position is plotted in the cross-sectional $R(t)$ plot of figure 4(b). The most noticeable difference is the deviation from linear growth kinetics. In addition, the $R(t)$ plot exhibits a sudden termination of growth, like that seen at higher feedstock pressures, but with a more pronounced retraction in the array length (~16%) after growth terminates, suggesting that the growing arrays are under stress.

Another noticeable difference is the slow initial growth regime (~6 min) shown in the inset of figure 4(b). At these pressures and flows in our reactor approximately 25 s is required for the feedstock gas to arrive at the Si substrate, which contributes to the initially slow kinetics [4]. In addition a slower nanotube nucleation and vertical alignment process at lower feedstock gas partial pressures can also result in the observed induction time.

The continually decreasing growth rate in figure 4(b) and the proven base growth mode of figures 2(a) and (b) implies feedstock-limited kinetics due to diffusion through the growing nanotube array. Diffusion-limited growth kinetics has been developed and applied in connection with thermal oxidation of silicon [21] and CVD growth of carbon nanotube arrays using ethylene as a feedstock gas at the relatively high partial pressures of ~160 Torr [20]. According to this model $R(t)$ is defined by the diffusion flux of the feedstock molecules through the array, $F_{\text{dif}} = -D(n_i - n_0)/R$, and the flux at the catalyst interface due to carbon nanotube growth, $F_{\text{tube}} = kn_i$, where D is the diffusion coefficient through a nanotube array, n_0 and n_i are the concentrations of feedstock gas at the top and the base of the array, respectively, R is the length of the array, and k is the effective rate constant for the conversion of feedstock gas into nanotubes. At stationary conditions when these two fluxes are equal and assuming that k is constant one

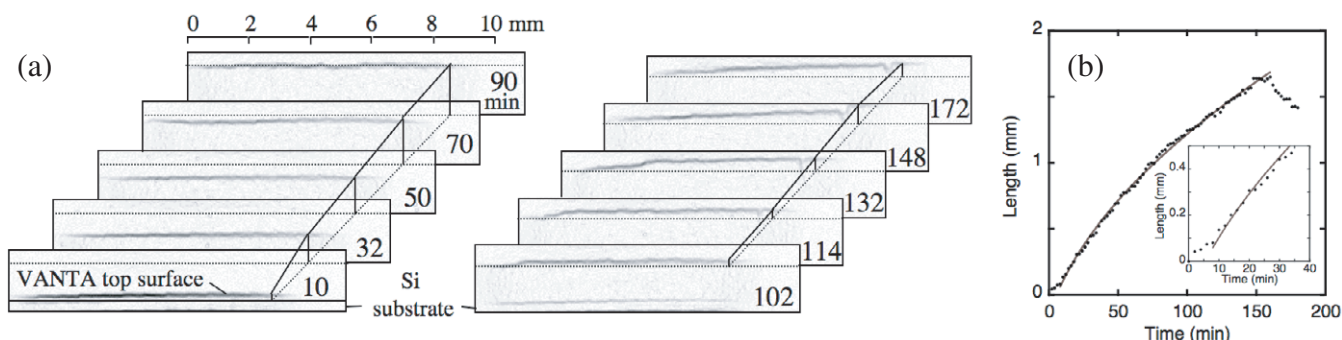


Figure 4. (a) A set of sequential frames (from 10 to 172 min) taken from a movie of growing VANTA array (available at stacks.iop.org/Nano/19/055605). Dotted horizontal lines are drawn close to the top of the array at the same distance from a Si substrate to help visualize the differences in the array lengths at different growth times. (b) The $R(t)$ plot (light circles) was measured at the cross-sectional position indicated by the black dotted line in figure 3(a). The growth conditions were identical to those described in figure 3 except the C_2H_2 flow that was 1.2 sccm. The black curve shows a fit to the data in the time interval from 5 to 150 min by equation (1) with the following fit parameters: $A = 0.14$ cm, $B = 5.5 \times 10^{-6}$ cm² s⁻¹, $t_0 = 328.3$ s. These parameters yield the diffusion coefficient, $D = 0.36$ cm² s⁻¹, ($n_0 = 3.85 \times 10^{15}$ molecules cm⁻³ which results in carbon density in the gas phase of 1.53×10^{-7} g cm⁻³ at the partial pressure of C_2H_2 of 0.4 Torr and $T = 730$ °C; the estimated density of VANTAs, $n_s \approx 0.02$ g cm⁻³) and the growth rate of the nanotube array at $t = t_0$, $v = kn_0/n_s = 4.1 \times 10^{-5}$ cm s⁻¹.

can obtain [21]:

$$R(t) = 0.5A\{[1 + 4B(t - t_0)/A^2]^{1/2} - 1\}, \quad (1)$$

where $A = 2D/k$, $B = 2Dn_0/n_s$, t_0 is the induction time, and n_s is the density of VANTAs. The fit to the experimental data using equation (1) shown by the solid line in figure 4(b) gives $D = 0.36$ cm² s⁻¹. The diffusion coefficient can be estimated using the theory of Knudsen diffusion through a porous medium [22] as $D = (2\varepsilon/3\tau)r\bar{v} = 0.16$ cm² s⁻¹, where $r \sim 30$ nm is the average radius of the cylindrical pores, $\bar{v} = 8 \times 10^4$ cm s⁻¹ is the mean molecular velocity of C_2H_2 molecules, $\varepsilon \sim 0.98$ is the porosity of VANTAS. Here we assumed that the tortuosity factor, τ , is close to 1 for the highly porous nanotube arrays.

From equation (1) one can conclude that the growth is diffusion limited when $(2n_s\bar{v}^2 t_{gr}/Dn_0) = \alpha \gg 1$, and is linear when $\alpha \ll 1$. The main factors that define the growth regime are the growth time, t_{gr} , that is defined by the time when the catalyst remains active, the initial growth rate, the diffusion coefficient, and the carbon densification factor, n_s/n_0 . For example, for the growth runs shown in figures 3(b) ($t_{gr} = 1200$ s) and 3(a) (curve 1, $t_{gr} = 2400$ s) $\alpha = 0.8$ and 0.6, respectively. In these cases, the $R(t)$ dependences are close to linear in the time interval from 0 to t_{gr} and the growth is not diffusion limited. For the run shown in figure 4(b) ($t_{gr} = 9000$ s), $\alpha \approx 5.5$ and the growth is diffusion limited. All three growth experiments were conducted at the same growth conditions, i.e. in flowing Ar (2000 sccm), H_2 (400 sccm), and C_2H_2 at the total pressure of 750 Torr and 730 °C except the C_2H_2 flow, which was maintained at 2.4 sccm for the first two cases and at 1.2 sccm for the third growth experiment. The decrease in C_2H_2 partial pressure resulted in much longer growth time and the longer nanotube array of ~ 1.5 mm (figure 4(b)) that increased α and shifted the growth conditions to the diffusion-limited case according to equation (1). The detailed nature of the feedstock gas transport through a nanotube array remains unclear, although several

different theories exist. These range from pure molecular transport controlled by elastic collisions with the nanotube walls, Knudsen diffusion [20] to chemisorption with possible dissociation of the feedstock molecules at the surface followed by surface diffusion along the nanotubes [1, 23]. Our results show that Knudsen diffusion through the nanotube arrays explains well the diffusion coefficients estimated from the experiment.

4. Conclusions

In summary, *in situ* videography of vertically aligned nanotube arrays grown to long lengths reveals different regimes for diffusion-limited growth and cooperative phenomena which tend to equilibrate the height of the arrays over lateral distances of several millimeters. Observations of the array heights versus time show that local regions of the array appear to have variable growth rates, i.e. pausing, resuming, and even retracting significantly (up to 16%) during a growth run. Laser irradiation of growing nanotube array tops during video imaging, coupled with subsequent SEM analysis, proved that growth in our experiments occurs from the base of the arrays. Laser irradiation was found to result in not only ablation, but an increase in apparent growth rate of the arrays. Possible reasons include: (i) changed catalyst activity, (ii) increased temperature, (iii) fracture of the array to allow less restricted gas diffusion to the catalyst at the base of the array, or (iv) a release in tension or straightening of the nanotubes in the array resulting in a faster apparent growth rate. The evolution in growth kinetics from constant to diffusion-limited behavior for feedstock partial pressures varying by just a factor of two was well-described in terms of a simple diffusion model [21].

Overall, the application of *in situ* videography to understand the growth of vertically aligned nanotube arrays reveals a more complex process than previously thought, with measured heights versus time reflecting both the growth and the retraction of the nanotubes in the array. Further *in situ* experiments are required to elucidate the forces inherent in

coordinated growth, the evolution of tension in the arrays and its possible feedback on the activity of the catalyst, and the effects of laser processing of catalysts on growth kinetics.

Acknowledgments

This work was supported by DOE Office of Basic Energy Sciences, Division of Materials Sciences and Engineering. The authors gratefully acknowledge the technical assistance of Pam Fleming, discussions with R F Wood, J C Wells, and S Pannala. Oak Ridge National Laboratory is managed and operated by UT-Battelle, LLC for the US Department of Energy under contract DE-AC05-00OR22725.

References

- [1] Louchev O A, Laude T, Sato Y and Kanda H 2003 *J. Chem. Phys.* **118** 7622
- [2] Futaba D N, Hata K, Yamada T, Mizuno K, Yumura M and Iijima S 2005 *Phys. Rev. Lett.* **95** 056104
- [3] Hata K, Futaba D N, Mizuno K, Namai T, Yumura M and Iijima S 2004 *Science* **306** 1362
- [4] Puztzky A A, Geohegan D B, Jesse S, Ivanov I N and Eres G 2005 *Appl. Phys. A* **81** 223
- [5] Wood R F, Pannala S, Wells J C, Puztzky A A and Geohegan D B 2007 *Phys. Rev. B* **75** 235446
- [6] Zhang M, Atkinson K P and Baughman R H 2004 *Science* **306** 1358
- [7] Zhang M, Fang S, Zhakhidov A A, Lee S B, Aliev A E, Williams C D, Atkinson K R and Baughman R H 2005 *Science* **309** 1215
- [8] Ivanov I N, Puztzky A A, Eres G, Wang H, Pan Z W, Cui H T, Jin R Y, Howe J and Geohegan D B 2006 *Appl. Phys. Lett.* **89** 223110
- [9] Cao A, Dickrell P L, Sawyer W G, Ghasemi-Nejhad M N and Ajayan P M 2005 *Science* **310** 1307
- [10] Rouleau C M, Eres G, Cui H, Christen H M, Puztzky A A and Geohegan D B 2008 *Appl. Phys. A* submitted
- [11] Baker R T K 1989 *Carbon* **27** 315
- [12] Helveg S, Lopez-Cartes C, Sehested J, Hansen P L, Clausen B S, Rostrup-Nielsen J R, Abild-Pedersen F and Norskov J K 2004 *Nature* **427** 426
- [13] Ichihashi T, Fujita J, Ishida M and Ochiai Y 2004 *Phys. Rev. Lett.* **92** 215702
- [14] Sharma R, Rez P, Treacy M M J and Stuart S J 2005 *J. Electron Microsc.* **54** 231
- [15] Lin M, Tan J P Y, Boothroyd C, Loh K P, Tok E S and Foo Y L 2006 *Nano Lett.* **6** 449
- [16] Geohegan D B, Puztzky A A, Ivanov I N, Jesse S, Eres G and Howe J Y 2003 *Appl. Phys. Lett.* **83** 1851
- [17] Kim D H, Jang H S, Kim C D, Cho D S, Yang H S, Kang H O, Min B K and Lee H R 2003 *Nano Lett.* **3** 863
- [18] Fan S S, Liu L and Liu M 2003 *Nanotechnology* **14** 1118
- [19] Liu K, Jiang K, Feng C, Chen Z and Fan S S 2005 *Carbon* **43** 2850
- [20] Zhu L, Hess D W and Wong C P 2006 *J. Phys. Chem.* **110** 5445
- [21] Deal B E and Grove A S 1965 *J. Appl. Phys.* **36** 3770
- [22] Mason E A and Malinauskas A P 1983 *Gas Transport in Porous Media: The Dusty Gas Model* (Amsterdam: Elsevier)
- [23] Louchev O A, Sato Y and Kanda H 2002 *Appl. Phys. Lett.* **80** 2752